ATTENUATION OF HOMOGENEOUS AND ISOTROPIC TURBULENCE BY SOLID PARTICLES

Wontae Hwang
Department of Mechanical Engineering,
Stanford University
Stanford, California 94305-3035, USA
wthwang@stanfordalumni.org

John K. Eaton
Department of Mechanical Engineering,
Stanford University
Stanford, California 94305-3035, USA
eaton@vk.stanford.edu

ABSTRACT

The interaction of a dilute dispersion of small heavy particles with homogeneous and isotropic air turbulence has been investigated. Stationary turbulence (at Taylor micro-scale Reynolds number of 230) with small mean flow was created in a nearly-spherical sealed chamber by means of eight synthetic jet actuators. Two-dimensional particle image velocimetry was used to measure fluid velocities in the presence of spherical glass particles that had diameters similar to the Kolmogorov length scale of the flow. The experiments were conducted in two different environments, the laboratory (with gravity) and NASA's KC-135 (without gravity). The laboratory experiments showed that the particles attenuated the fluid turbulence kinetic energy (up to 35 – 40%) and viscous dissipation rate (up to 40 – 50%) with increasing mass loadings (up to 30%). The micro-gravity experiments showed that the absence of particle potential energy loss and particle wakes caused greater levels of turbulence attenuation since there was no additional production due to mean particle motion.

1. INTRODUCTION

Particle-laden turbulent flows are prevalent in industrial and natural environments. Examples include fast fluidized beds, pollution abatement systems, and volcanic ash eruptions. Under certain conditions, the turbulence levels of the carrier phase can be attenuated (up to 80% in some cases), even at negligible volume fractions of particles. The underlying physics of this phenomenon are still not well understood. There is a need for experiments in simple flows to increase the understanding of this phenomenon and to create a database for model developers.

Homogeneous and isotropic turbulence is the most basic type of turbulence, but it has been difficult to create in the laboratory. Stationary homogeneous turbulence self-induced by settling particles was investigated by Parthasarathy and Faeth (1990), Mizukami et al. (1992), and Chen et al. (2000). Grid-generated turbulence has also been examined by Schreck and Kleis (1993) and Geiss et al. (2004). Many researchers have attempted to use direct numerical simulations (DNS) with point forces representing the particles to study homogeneous and isotropic turbulence. Squires and Eaton (1990) and Boivin et al. (1998) examined stationary turbulence, while Elghobashi and Truesdell (1993), Druzhinin and Elghobashi (1999), and Sundaram and Collins (1999) investigated decaying turbulence. Maxey et al. (1997) used Gaussian envelopes centered on the particles to represent the particle force fields. Burton and Eaton (2003) conducted 'true' DNS by fully resolving the flow around a single particle. Since DNS is still computationally expensive, Boivin et al. (2000) recently used large eddy simulations (LES) to examine the fluid-particle energy exchange in stationary turbulence.

The objective of this study was to experimentally investigate the ideal case of a uniformly dispersed array of heavy particles interacting with stationary homogeneous and isotropic air turbulence in the absence of mean flow (fluid velocity, $\mathbf{u} = \mathbf{u}'$). The experiments were conducted in two different environments. The first set of experiments was conducted in the lab with particles falling through the turbulence at a certain settling velocity (particle velocity, $\mathbf{v} = \mathbf{v}_t + \mathbf{v}'$). The second set of experiments was conducted in micro-gravity to create a nearly stationary dispersion of particles ($\mathbf{v} = \mathbf{v}'$) and eliminate the mean particle wakes. The following specific conditions were considered. The particle diameter $d_p \sim \eta_k$ (Kolmogorov length scale), particle-to-fluid density ratio $\rho_p/\rho_f \sim 2000$, particle Stokes number (based on the Kolmogorov time scale) $St_k \sim 50$, and particle Reynolds number $Re_p \sim 10$. The flow had maximum particle volume concentration $\alpha_p \sim 10^{-4}$, mass loading $\phi \sim 0.3$, and total number of particles $N_p \sim 5 \times 10^6$, which corresponded to inter-particle spacing $l_p \sim 15 d_p$.

2. FLOW FACILITY AND MEASUREMENT TECHNIQUES

2.1. Experimental Setup and Procedures in the Lab

The experiments were conducted in a turbulence chamber, which is documented in Hwang and Eaton (2004). It is a 410 mm^3 symmetric Plexiglas box with the corners cut off to make it approximately internally spherical. The turbulence was generated by synthetic jet actuators which were mounted on the eight corners. The actuators used 165 mm

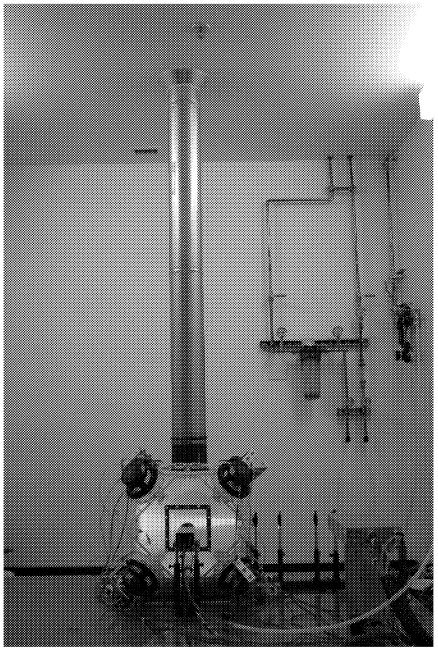

Figure 1: Experimental setup. *Counter-clockwise from top*: particle chute, turbulence chamber, Kodak ES1.0/10 camera, PIV Nd:YAG laser, and sheet-creating optics.

polypropylene cone Pioneer woofers, which made them robust and optimal for particle-laden flow studies. Random frequency (between 90 and 110 Hz) and phase sine waves were individually amplified by a Phast PLB-Amp8 power amplifier and sent to the speakers. The synthetic jets passed through ejector tubes which increased the flow and decreased the velocity of the jet. Wire mesh was attached to the end of the ejector tubes as turbulence grids to introduce intermediate scales into the jet.

Glass particles 165 μm in diameter were fed from a screw feeder located on the roof of the lab and dispersed by five equally-spaced sieves. A honeycomb followed to reduce horizontal motion caused by the screens. The particles then fell through a 152 mm diameter, 2.5 m long chute which reached from the roof down through the ceiling to the top of the chamber. The chute was long enough for the particles to reach their terminal velocity before entering the chamber. The experimental setup is depicted in figure 1.

A fluidized bed seeder was used in conjunction with a cyclone separator to seed the flow with 0.3 μm deagglomerated alumina particles. The air was filtered before exiting the chamber. The chamber was always seeded prior to (not during) data acquisition.

The experiments were conducted by taking a set of unladen flow measurements before each particle-laden flow run to compare and normalize results. A second unladen flow data set was acquired after the end of the laden-flow measurements to determine how the unladen flow recovered with particles accumulated on the bottom of the chamber. Each data set (pre-unladen, laden, post-unladen) consisted of 1000 image pairs. Three different ϕ up to 30% and two different turbulence levels (twice the turbulence kinetic energy, $q^2_{\phi=0} = 1.4$ m^2 s^{-2} and $q^2_{\phi=0} = 1.1$ m^2 s^{-2}) were tested.

Figure 2: Free-floating rack in micro-gravity.

2.2. Experimental Setup and Procedures in Micro-Gravity

The micro-gravity experiments were conducted on NASA's KC-135, which flies in parabolic trajectories to create a reduced-gravity environment. The electronic devices were fixed on a stationary rack and bolted to the cabin floor, while the main apparatus (which housed the turbulence chamber, particle image velocimetry system, and accelerometer) was free-floated, as shown in figure 2. Before each flight, a new set of 160 μm glass particles corresponding to a certain mass loading was put into the turbulence chamber. The chamber was seeded as the plane was climbing at 2 g, and laden-flow data were acquired as the plane dived into micro-gravity. Results were compared with unladen flow measurements taken on the ground at the same experimental conditions.

2.3. Measurement System and Techniques

Two-dimensional particle image velocimetry (PIV) measurements were obtained at the center of the chamber in a 40×40×0.5 mm^3 region. A Continuum Minilite PIV dual-head Nd:YAG laser (25 mJ/pulse at 532 nm) and Kodak ES1.0/10 10 bit CCD (1018 × 1008 resolution) camera were triggered by LabVIEW. Image acquisition was achieved with an EPIX PIXCI-D frame grabber board and 450 MHz Pentium II desktop computer.

Continuous-phase measurements were the main focus of this study. To obtain accurate PIV results, the dispersed phase was first eliminated from the images using a spatial median filtering technique proposed by Kiger and Pan (2000). The images of tracers were then processed using a PIV algorithm written in Matlab by Han (2001), which incorporated recursive interrogation window offset and reduction to increase the spatial resolution and accuracy. The final iteration used a window size of 32 × 32 pixels at 50% overlap, resulting in a velocity vector field of 59 × 59 vectors. The images were processed with a 2.2 GHz Intel Xeon dual-processor workstation at 30 s per image pair.

3. TURBULENCE MODIFICATION IN THE PRESENCE OF GRAVITY

The homogeneity and isotropy of the base unladen flow has previously been qualified by Hwang and Eaton (2004) and will not be presented here. Only results from the particle-laden flow experiments will be presented.

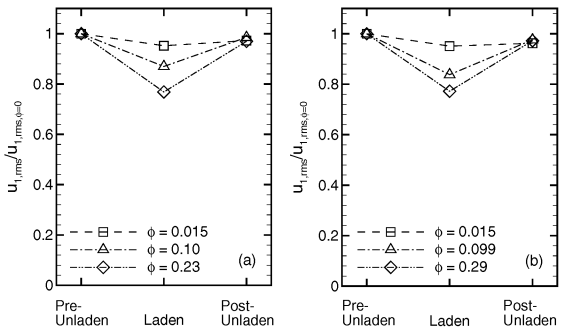

Figure 3: Example of procedure of the lab experiments. Variation of $u_{1,rms}$ with addition of particles for cases (a) $q^2_{\phi=0} = 1.4$ m^2 s^{-2} and (b) $q^2_{\phi=0} = 1.1$ m^2 s^{-2}.

3.1. Turbulence Kinetic Energy and Dissipation

Flow statistics were normalized by corresponding results from each pre-unladen data set. By plotting the normalized statistics as sequential data points corresponding to pre-unladen, laden, and post-unladen data sets, we could see how the flow recovered back to its original state after particles had accumulated on the bottom of the chamber. Figure 3 shows an example of this experimental procedure for the horizontal fluctuating velocity. As ϕ is increased, $u_{1,rms}$ is attenuated, and almost recovers to its original pre-unladen value for both turbulence levels. The vertical fluctuating velocity showed the same trend.

The reduction in fluctuating velocities corresponded to attenuation of turbulence kinetic energy (TKE). Figure 4(a) shows that q^2 decreased monotonically with increasing particle mass loading for both turbulence levels. Attenuation levels reached almost 40% for the highest mass loadings of $\phi = 0.23$ ($q^2_{\phi=0} = 1.4$ m^2 s^{-2} case) and 0.29 ($q^2_{\phi=0} = 1.1$ m^2 s^{-2} case). The amount of attenuation was significantly greater than that of the DNS studies of particle-laden homogeneous and isotropic turbulence shown in figure 4(a). This suggests that the particle point-force coupling scheme used in most numerical simulations does not capture all of the physics, resulting in underestimation of the actual amount of turbulence attenuation.

The attenuation of ϵ with particle mass loading is shown in figure 4(b). Attenuation levels were similar for both turbulence levels, and reached 40 – 50% for the highest mass loadings. This was slightly higher than the attenuation levels of the turbulence kinetic energy. It is interesting to note that ϵ was attenuated similarly for the stationary turbulence studies of Squires and Eaton (1990) and Boivin et al. (1998), while it was slightly augmented for the decaying turbulence studies of Elghobashi and Truesdell (1993) and Sundaram and Collins (1999). The decrease in ϵ resulted in an increase of the Kolmogorov time and length scales.

3.2. Two-point Spatial Velocity Correlations

Two-point longitudinal velocity correlations were plotted for different ϕ and compared to the average correlation coefficient of the pre-unladen data sets in figure 5 for the higher energy case. The separation distance was normalized by the

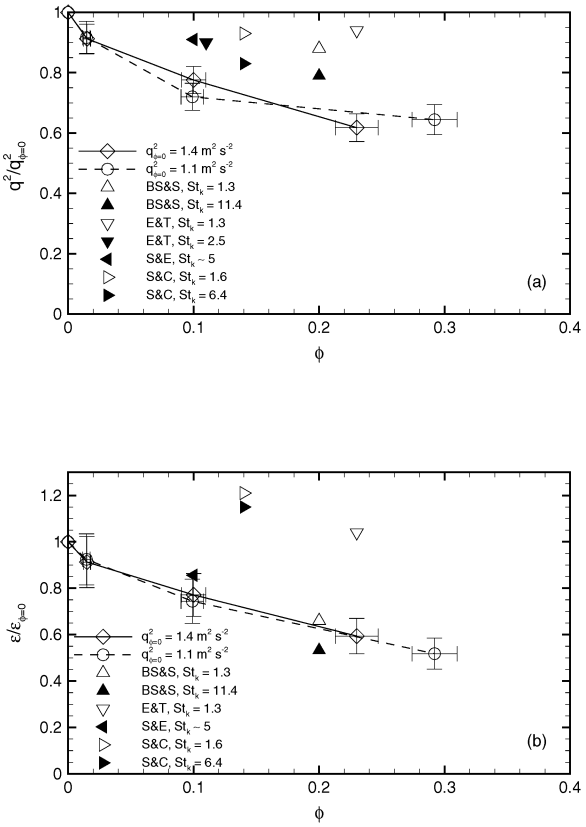

Figure 4: Attenuation of (a) TKE and (b) ϵ with addition of particles. Compared with DNS data from Boivin et al. (1998), Elghobashi and Truesdell (1993), Squires and Eaton (1990), and Sundaram and Collins (1999).

average Kolmogorov length scale of the three pre-unladen data sets. As increasing amounts of particles were dropped through the flow, the longitudinal correlation of the horizontal fluctuating velocities in figure 5(a) did not deviate from the average pre-unladen curve. That is, there was no significant distortion of the turbulence structure evident in this correlation by particles. On the other hand, the longitudinal correlation increased at large separation distances and decreased at small separation distances (as shown in the close-up in the insert) for the vertical fluctuating velocities (figure 5b). The increase at large separation distances could possibly have been due to clusters of particles transferring energy to the flow via local jet-like fluid motion as they settled. The decrease at small separation distances corresponded to a decrease in the Taylor microscale and suggested that individual particles extracted energy through small-scale extra dissipation near the particle surface. Similar trends were observed for the lower energy case.

3.3. Energy Spectra

The radial energy spectra are shown in figure 6 for the higher energy case. The wavenumber was normalized by the average pre-unladen Kolmogorov length scale, and the average pre-unladen spectrum is shown for comparison. In-

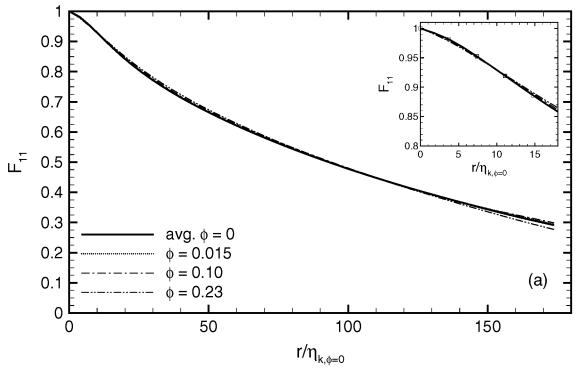

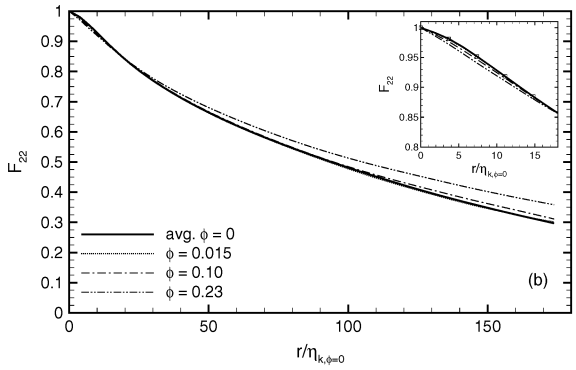

Figure 5: Two-point longitudinal velocity correlations of the particle-laden flow for the higher energy case in the (a) horizontal and (b) vertical directions.

creasing the mass loading of particles increasingly attenuated the horizontal component of the spectrum (figure 6a). The attenuation was fairly uniform across all wavenumbers. The attenuation for the vertical component was fairly uniform at lower wavenumbers, but decreased at higher wavenumbers (figure 6b). This suggests that spectral cross-over might have occurred at higher wavenumbers beyond those resolved here (see e.g. Squires and Eaton, 1990; Boivin et al., 1998; Sundaram and Collins, 1999). The vertical component also had larger energy than the horizontal component, indicating that the flow was not as isotropic as before. This was probably due to the vertical particle wakes and local jets induced by particle clusters.

3.4. Energy Budget

To help understand the coupling between the particles and turbulence, an energy budget analysis of the turbulent flow was conducted, taking the $40 \times 40 \times 0.5$ mm^3 measurement domain as the control volume. Assuming an overall steady-state process for the fluid in the control volume, the energy budget for the fluid-phase kinetic energy could be written as

$$\dot{E}_{i,sja} + \phi g v_t - \dot{E}_s = 0 \qquad (1)$$

The first term $\dot{E}_{i,sja}$ represents the net rate of energy input into the control volume by transport and diffusion of turbu-

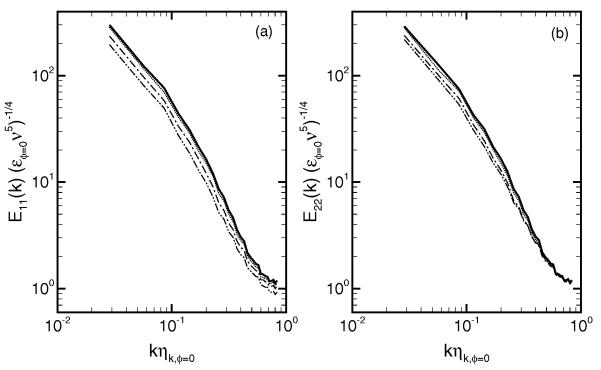

Figure 6: Radial energy spectra of the particle-laden flow for the higher energy case for the (a) horizontal and (b) vertical velocity components: ———, avg. $\phi = 0$; ·····, $\phi = 0.015$; —·—, $\phi = 0.10$; —··—, $\phi = 0.23$.

lence kinetic energy from the synthetic jet actuators. The second term $\phi g v_t$ (where g is gravitational acceleration and v_t is the settling velocity of particles in the turbulence) is an input of energy into the fluid in the control volume due to the particles falling at a certain settling velocity and losing gravitational potential energy. This energy appeared as wakes of individual particles and as local jets produced by falling particle clusters. Some of this potential energy was dissipated directly by viscous effects near the particle surface at scales significantly smaller than the smallest turbulent eddies (refer to the "extra dissipation due to particles" term below). The third term in (1), $\dot{E}_s$, is the rate of energy sink (or viscous dissipation), that we choose to split for discussion's sake into two components, the ordinary viscous dissipation of turbulence energy and the extra dissipation due to particles. The normal viscous dissipation in single-phase flow is a result of the turbulence cascade from large-scale energy-containing eddies to smaller dissipating scales. The extra dissipation due to particles is the viscous dissipation due to small-scale motions in the vicinity of particles, and can also be described as "unresolved dissipation." In one sense, both the ordinary viscous dissipation and the extra dissipation due to particles are different manifestations of the same physical mechanism. However, the extra dissipation occurs mostly at scales smaller than those produced by the turbulence cascade, and was not resolved in our measurements. In that sense, these two dissipation rates may be thought of as separate energy sinks.

Large-scale flow distortions might also have been produced by individual particles and particle clusters as they fell through the flow. There are two ways to view the effects of these flow distortions. The first approach is to assume that the flow distortions are at the same length scale as and indistinguishable from the regular turbulence, considering that the average inter-particle spacing was approximately $15\eta_k$. The dissipation for these flow distortions would be accounted for in the measurements of the viscous dissipation. That means the extra dissipation due to particles would be manifested as the only energy sink caused by the particles. Equation (1) could then be written as

$$\dot{E}_{i,sja} + \phi g v_t - \epsilon - \epsilon_p = 0 \qquad (2)$$

where ϵ is the resolved dissipation rate and ϵ_p is the extra dissipation rate due to particles.

The value of each term in (2) was estimated from the consecutive pre-unladen and laden data sets for the higher energy case corresponding to the highest mass loading of $\phi = 0.23$. It was difficult to directly measure the energy input rate from the speakers, so it was indirectly estimated from the viscous dissipation rate in the pre-unladen data set, assuming that the energy transported from the synthetic jet actuators was all dissipated:

$$\dot{E}_{i,sja} = \epsilon_{\phi=0} \tag{3}$$

This value was 4.26 $m^2\ s^{-3}$. The production in the fluid due to the loss of potential energy of the particles was 1.34 $m^2\ s^{-3}$ for $\phi = 0.23$ and $v_t = 0.59\ m^2\ s^{-1}$. The viscous dissipation rate for the particle-laden data set was measured to be 2.50 $m^2\ s^{-3}$. The extra dissipation due to particles could thus be estimated by difference as 3.10 $m^2\ s^{-3}$.

The standard model that has been used to estimate this extra dissipation (Elghobashi and Abou-Arab, 1983; Rogers and Eaton, 1991) for unresponsive, large St_k particles can be written as

$$\epsilon_p \cong \frac{\overline{c}}{\rho_f \tau_{p,s}} \left(\overline{u_i' u_i'}\right) \tag{4}$$

where $\overline{c}$ denotes the mean particle concentration, and $\tau_{p,s}$ is the Stokes particle time constant. This extra dissipation was estimated to be 0.32 $m^2\ s^{-3}$, nearly an order of magnitude smaller than the estimated value of 3.10 $m^2\ s^{-3}$ from (2). The reason for this discrepancy could be due to the fact that (4) often underpredicts ϵ_p. The assumptions employed to obtain (4) are essentially the same ones used to develop point-force coupled simulation codes. Segura et al. (2004) recently showed evidence that such codes underpredict ϵ_p by about an order of magnitude.

The second approach assumes that the particles distort the flow in such a way that the large energetic eddies are greatly disturbed. This idea may seem feasible if one considers the particles as a series of screens with an average mesh spacing of $15\eta_k$ continuously falling through the turbulence. Not only do the particles add turbulence to the flow through particle wakes, but the energetic flow structure can be destroyed by this "screen effect". Considering the fact that particle clusters 10 – 20 mm wide sometimes fell through the turbulent flow which had an integral length scale of approximately 80 mm, this seems even more plausible. This destruction in flow structure would have to be accounted for as a sink separate from ϵ_p, as the viscous dissipation that is measured only takes into account the turbulent energy that is being cascaded down to smaller scales from the disturbed flow. $\dot{E}_s$ would thus be written as

$$\dot{E}_s = \epsilon + \epsilon_p + \dot{E}_{s,se} \tag{5}$$

where $\dot{E}_{s,se}$ is the energy sink due to this "screen effect." It is not clear how large this term would be compared to ϵ_p, but the sum $\epsilon_p + \dot{E}_{s,se}$ should be 3.10 $m^2\ s^{-3}$ from (2).

It is unclear as to which approach describes the large-scale flow distortions more accurately. The energy sink due to particles is possibly a combination of both effects.

4. TURBULENCE MODIFICATION IN THE ABSENCE OF GRAVITY

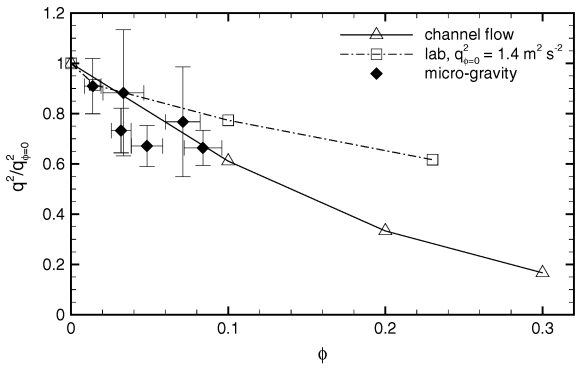

Figure 7: Attenuation of TKE in micro-gravity. Results are compared with the channel flow centerplane data of Paris and Eaton (2001) and the higher energy case obtained in the lab.

The number of valid experimental data sets taken on the micro-gravity flights were limited due to various technical difficulties. Data were deemed invalid after the free-floating rack hit the ceiling or wall of the plane, or if the NASA technicians grabbed it when its trajectory appeared dangerous. There were also problems with particle dispersion as the particles would stick to the chamber floor due to electrostatic forces, get stuck in the corners, and also find their way into the synthetic jet actuator plenums. Even though the TKE was spatially averaged for all the measurement locations corresponding to velocity vector positions, the small number of image pairs available for each data set corresponded to a large uncertainty. Each image pair is an instantaneous realization of the flow field, and a few realizations does not give a good statistical representation of the turbulence.

A general trend of decreasing TKE with increasing mass loading could nevertheless still be detected (figure 7). It is interesting to note that the data seemed to follow the trend of the turbulent channel flow centerplane data of Paris and Eaton (2001), where the turbulence was approximately homogeneous and isotropic and the TKE was diffused toward the centerplane from near the wall. The TKE was also attenuated more in micro-gravity than in the laboratory (only the higher energy case is shown for clarity). This is an indication that the absence of particle wakes and local jets caused by settling particle clusters enhanced the effects of turbulence attenuation, as no extra energy was added to the flow. The attenuation was probably due to the extra dissipation by particles or the flow structure distortion caused by the "screen effect" of particles.

5. SUMMARY

Modulation of homogeneous and isotropic turbulence by a dilute ($\alpha_p \sim 10^{-4}$) dispersion of small ($d_p \sim \eta_k$) heavy ($\rho_p/\rho_f \sim 2000, St_k \sim 50$) particles was experimentally investigated. Eight synthetic jet actuators mounted around a nearly-spherical chamber created stationary turbulence (at $Re_\lambda \sim 230$) with small mean flow at the center. Two-dimensional PIV was used with spatial median filtering (Kiger and Pan, 2000) to separate the glass particles and tracers in the images. Gas-phase measurements were obtained from the separated tracer images. The experiments were conducted in two different environments, with and without gravity.

The laboratory experiments showed that the turbulence kinetic energy and viscous dissipation rate were attenuated with increasing ϕ. At the highest mass loadings, attenuation levels reached 35 – 40% for TKE and 40 – 50% for ϵ. The longitudinal spatial velocity correlation did not change with the addition of particles for the horizontal fluctuating velocities, but increased at large separation distances and decreased at small separation distances for the vertical velocities. The radial energy spectra showed increasing attenuation of the horizontal component with increasing mass loading, with the attenuation being uniform across all measurable wavenumbers. The vertical component had fairly uniform attenuation at lower wavenumbers, but the amount of attenuation decreased at higher wavenumbers. It also had higher energy compared to the horizontal component, indicating that the level of isotropy had decreased. All of the results and trends were similar for both turbulence levels.

The main source of gas-phase energy production in the chamber was the synthetic jet actuators. The loss of potential energy of the settling particles also produced an appreciable amount of extra turbulence kinetic energy for the flow. The micro-gravity experiments confirmed this, as the TKE was attenuated more in the absence of particle wakes and local jets caused by settling particle clusters. The sink of energy in the chamber was due to the ordinary fluid viscous dissipation and an energy sink caused by particles. The energy sink due to particles had contributions from "unresolved" dissipation caused by small-scale velocity disturbances near the particles, ϵ_p, and dissipation caused by large-scale flow distortions from particle wakes and particle clusters, which could possibly have been accounted for in the fluid viscous dissipation. The standard model that is used to estimate the "unresolved" extra dissipation (Elghobashi and Abou-Arab, 1983; Rogers and Eaton, 1991) greatly underestimated this term.

ACKNOWLEDGEMENTS

We would like to acknowledge the support of the National Aeronautics and Space Administration, which sponsored this research through grant numbers NCC3-640 and NAG3-2738 under the supervision of Dr. Nasser Rashidnia. We are also grateful for the help of Eon-Soo Lee, Dr. Christopher Elkins, and Patrick Cabral in conducting the experiments.

REFERENCES

Boivin, M., Simonin, O., and Squires, K. D., 1998, "Direct Numerical Simulation of Turbulence Modulation by Particles in Isotropic Turbulence," *J. Fluid Mech.*, Vol. 375, pp. 235-263.

Boivin, M., Simonin, O., and Squires, K. D., 2000, "On the Prediction of Gas-Solid Flows with Two-Way Coupling using Large Eddy Simulation," *Phys. Fluids*, Vol. 12, pp. 2080-2090.

Burton, T. M., and Eaton, J. K., 2003, "Fully Resolved Simulations of Particle-Turbulence Interaction," Technical Report TSD-151, Stanford Univ., Stanford, CA.

Chen J.-H, Wu, J.-S., and Faeth, G. M., 2000, "Turbulence Generation in Homogeneous Particle-Laden Flows," *AIAA J.*, Vol. 38, pp. 636-642.

Druzhinin, O. A., and Elghobashi, S., 1999, "On the Decay Rate of Isotropic Turbulence Laden with Microparticles," *Phys. Fluids*, Vol. 11, pp. 602-610.

Elghobashi, S. E., and Abou-Arab, T. W., 1983, "A Two-Equation Turbulence Model for Two-Phase Flows," *Phys. Fluids*, Vol. 26, pp. 931-938.

Elghobashi, S., and Truesdell, G. C., 1993, "On the Two-Way Interaction Between Homogeneous Turbulence and Dispersed Solid Particles. I: Turbulence Modification," *Phys. Fluids* A, Vol. 5, pp. 1790-1801.

Geiss, S., Dreizler, A., Stojanovic, Z., Chrigui, M., Sadiki, A., and Janicka, J., 2004, "Investigation of Turbulence Modification in a Non-Reactive Two-Phase Flow," *Exp. Fluids*, Vol. 36, pp. 344-354.

Han, D., 2001, "Study of Turbulent Nonpremixed Jet Flames Using Simultaneous Measurements of Velocity and CH Distribution," Technical Report TSD-134, Stanford Univ., Stanford, CA.

Hwang, W., and Eaton, J. K., 2004, "Creating Homogeneous and Isotropic Turbulence without a Mean Flow," *Exp. Fluids*, Vol. 36, pp. 444-454.

Kiger, K. T., and Pan, C., 2000, "PIV Technique for the Simultaneous Measurement of Dilute Two-Phase Flows," *J. Fluids Eng.*, Vol. 122, pp. 811-818.

Maxey, M. R., Patel, B. K., Chang, E. J., and Wang, L.-P., 1997, "Simulations of Dispersed Turbulent Multiphase Flow," *Fluid Dynamics Research*, Vol. 20, pp. 143-156.

Mizukami, M., Parthasarathy, R. N., and Faeth, G. M., 1992, "Particle-Generated Turbulence in Homogeneous Dilute Dispersed Flows," *Int. J. Multiphase Flow*, Vol. 18, pp. 397-412.

Paris, A. D., and Eaton, J. K., 2001, "Turbulence Attenuation in a Particle-Laden Channel Flow," Technical Report TSD-137, Stanford Univ., Stanford, CA.

Parthasarathy, R. N., and Faeth, G. M., 1990, "Turbulence Modulation in Homogeneous and Dilute Particle-Laden Flows," *J. Fluid Mech.*, Vol. 220, pp. 485-514.

Rogers, C. B., and Eaton, J. K., 1991, "The Effect of Small Particles on Fluid Turbulence in a Flat-Plate, Turbulent Boundary Layer in Air," *Phys. Fluids* A, Vol. 3, pp. 928-937.

Schreck, S., and Kleis, S., 1993, "Modification of Grid-Generated Turbulence by Solid Particles," *J. Fluid Mech.*, Vol. 249, pp. 665-688.

Segura, J. C., Eaton, J. K., and Oefelein, J. C., 2004, "Predictive Capabilities of Particle-Laden Large Eddy Simulation, Technical Report TSD-156, Stanford Univ., Stanford, CA.

Squires, K. D., and Eaton, J. K., 1990, "Particle Response and Turbulence Modification in Isotropic Turbulence," *Phys. Fluids* A, Vol. 2, pp. 1191-1203.

Sundaram, S., and Collins, L. R., 1999, "A Numerical Study on the Modulation of Isotropic Turbulence by Suspended Particles," *J. Fluid Mech.*, Vol. 379, pp. 105-143.